Developmental Cognitive Neuroscience 50 (2021) 100977

Contents lists available at ScienceDirect

Developmental Cognitive Neuroscience

journal homepage: www.elsevier.com/locate/dcn

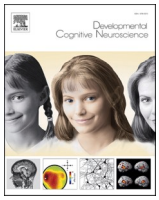

Perception-action integration in young age—A cross-sectional EEG study

Roxane Dilcher [a,1], Christian Beste [b,1,*], Adam Takacs [b], Annet Bluschke [b], Eszter Tóth-Fáber [c,d], Maximilian Kleimaker [e], Alexander Münchau [e,2], Shu-Chen Li [a,f,2,**]

[a] Chair of Lifespan Developmental Neuroscience, Faculty of Psychology, TU Dresden, Germany
[b] Cognitive Neurophysiology, Department of Child and Adolescent Psychiatry, Faculty of Medicine, TU Dresden, Germany
[c] Doctoral School of Psychology, ELTE Eötvös Loránd University, Budapest, Hungary
[d] Institute of Psychology, ELTE Eötvös Loránd University, Budapest, Hungary
[e] Institute of Systems Motor Science, University of Lübeck, Germany
[f] Centre for Tactile Internet With Human-in-the-Loop, TU Dresden, Germany

ARTICLE INFO

Keywords:
Event file coding
EEG
Cognitive
Control
Perception-action binding
Child and adolescent development
Functional neuroanatomy

ABSTRACT

Humans differ in their capacity for integrating perceived events and related actions. The "Theory of event coding" (TEC) conceptualizes how stimuli and actions are cognitively bound into a common functional representation (or "code"), known as the "event file". To date, however, the neural processes underlying the development of event file coding mechanisms across age are largely unclear. We investigated age-related neural changes of event file coding from late childhood to early adulthood, using EEG signal decompositions methods. We included a group of healthy participants (n = 91) between 10 and 30 years, performing an event file paradigm. Results of this study revealed age-related effects on event file coding processes both at the behavioural and the neurophysiological level. Performance accuracy data showed that event file unbinding und rebinding processes become more efficient from late childhood to early adulthood. These behavioural effects are reflected by age-related effects in two neurophysiological subprocesses associated with the superior parietal cortex (BA7) as revealed in the analyses using EEG signal decomposition. The first process entails mapping and association processes between stimulus and response; whereas, the second comprises inhibitory control subprocesses subserving the selection of the relevant motor programme amongst competing response options.

1. Introduction

In cognitive neuroscience research, understanding the mechanisms underlying cognitive control and response selection during perception and action is of great importance. **The term cognitive control can be regarded to be synonymous to executive functions (**Diamond, 2013), albeit there are nuances between these definitions (Nigg, 2017) and multiple facets of cognitive control processes can be distinguished (Diamond, 2013; Freund et al., 2021**). Several lines of evidence suggest that that cognitive control processes are subject to profound developmental changes across childhood and young adulthood in typical populations (e.g.,** Friedman et al., 2009; Luna, 2009; Luna et al., 2010; Marek et al., 2015; Munakata et al., 2012; Vedechkina and Borgonovi, 2021**), which are also of relevance for developmental neuropsychiatric disorders (**Arnsten and Rubia, 2012; McTeague et al., 2017; Nigg, 2017**). However, a common theme that runs through all these lines of research is the tenet that cognitive control relates to the processes of translating a specific stimulus input to an appropriate** behavioral **output in a given task context. What is thus central for any form of cognitive control and its development is how stimulus input becomes associated with a particular response and how this association is then represented (**Freund et al., 2021**). A prominent conceptual framework addressing** how perceived events (i.e., perceptual processes) and related response actions (i.e., sensorimotor processes) are integrated and represented in the brain **is** the "Theory of Event Coding" (TEC). **TEC** conceptualizes how

* Corresponding author at: Cognitive Neurophysiology, Department of Child and Adolescent Psychiatry, Faculty of Medicine, TU Dresden, Fetscherstrasse 74, 01307 Dresden, Germany.
** Corresponding author at: Lifespan Developmental Neuroscience, Faculty of Psychology, TU Dresden, Zellescher Weg 17, 01062 Dresden, Germany.
E-mail addresses: christian.beste@uniklinikum-dresden.de (C. Beste), shu-chen.li@tu-dresden.de (S.-C. Li).
[1] Shared first authorship.
[2] Shared senior authorship.

https://doi.org/10.1016/j.dcn.2021.100977
Received 10 January 2021; Received in revised form 26 April 2021; Accepted 15 June 2021
Available online 17 June 2021

perception-related stimulus features and representations of action planning as well as implementation are stored and represented in a common functional network (Hommel et al., 2001). In particular, TEC proposes that the perception of an object triggers a specific corresponding response, since the binding of object features (e.g. orientation, colour, or location) with response actions (e.g. right or left finger movement) results in the creation of a transient, episodic "event file", which is the mental representation of stimulus features and the accompanying action (Hommel, 1998). Once an event file has been formed, it is automatically activated whenever the corresponding stimulus or response is re-encountered (Hommel et al., 2001). This "modus operandi" of event coding affects the way responses are successfully selected and carried out. In cases where the same stimuli require the execution of different responses, previously created stimulus-response associations in an event file may cause difficulties because earlier bindings and related expectancies are only partially met. As a result, the preestablished event file has to be updated, leading to "partial repetition costs" that are commonly reflected in longer reaction times (RTs) and higher error rates. In contrast, whenever at least one stimulus (or one stimulus feature of an object) is repeated and requires the same response as before, pre-established bindings facilitate subsequent responses, leading to "partial repetition benefits" (Colzato et al., 2006; Frings et al., 2020; Hommel, 1998; Hommel et al., 2001).

Event files are not represented by individual neurons or local neural populations but by widely distributed networks (Hommel, 2009; Kikumoto and Mayr, 2020; Takacs et al., 2020a). Past studies using neurophysiological methods have shown that the creation and updating of stimulus-response bindings in event files require the integration of information processing across distant brain areas, particularly of regions in the inferior and parietal cortex (Kikumoto and Mayr, 2020; Petruo et al., 2019, 2016; Takacs et al., 2020a, 2020b). Processes underlying event file coding can be modulated by the dopaminergic system (Colzato et al., 2007a, 2007b, 2012, 2013; Colzato and Hommel, 2008). For instance, spontaneous eyeblinks, affect-inducing pictures and cannabis consumption (i.e. factors related to the activation of the dopaminergic system) have been associated with cognitive control and binding strength assessed with event-file paradigms (Colzato et al., 2007b, 2007a; Colzato and Hommel, 2008). Later studies emphasized the role of striatal dopaminergic pathways for event coding, because binding strength was predicted by polymorphisms of the dopamine transporter gene DAT1 and by dopaminergic medication in patients with Parkinson's disease (Colzato et al., 2013, 2012). Both the importance of distributed brain activity mediated via long-range connections and the role of the dopamine system are of direct relevance to developmental dynamics affecting event file coding.

Cognitive development across the lifespan is associated with neuroanatomical and neurochemical network changes (Bäckman et al., 2006; Hämmerer et al., 2014; Li, 2012; Li et al., 2006). There is ample evidence showing that prefrontal and parietal cortices develop rather gradually during childhood and adolescence (Andre et al., 2016; Crone, 2014; Crone and Steinbeis, 2017; Darki and Klingberg, 2015; Luna et al., 2010; Ofen et al., 2012; Shing et al., 2010; van Duijvenvoorde et al., 2016). The protracted development of the frontal-parietal circuitries at the level of cortical networks is also accompanied by the late maturation of cortical dopaminergic modulation. The efficacy (e.g. the availability of dopamine synthesis or dopamine receptor protein) of subcortical and cortical dopamine systems shows a lead-lag pattern during typical development (see Li, 2012 for review). Using positron emission tomography (PET) imaging to measure dopamine receptor functions in vivo, a study by Jucaite et al. (2010) showed that dopamine D1 receptor function in the prefrontal cortex displays a gradual age-dependent development until late adolescence; in contrast, D1 receptor function in subcortical regions (i.e., dorsal or ventral striatum) reaches adult level already in late childhood/early adolescence.

At the functional level, previous research has shown that the maturation of the frontal and parietal networks parallel and contribute to the development of working memory and related executive control functions, such as task switching (Crone and Richard Ridderinkhof, 2011; Karbach et al., 2011; Kray et al., 2008), as well as the development of intentional memory organization processes that help bind together different to-be-remembered items of a memory episode (e.g., Li et al., 2006; Shing et al., 2010). Of particular relevance for the current study, previous work points to task-switching and action control deficits in childhood, as reflected in greater effects associated with action execution and reliance on stimulus-response associations (Crone et al., 2006; Karbach et al., 2011; Kray et al., 2008). Environmental supports, such as verbal labelling, seem to enhance associations between task-relevant features and event representation, therefore are helpful for reducing children's action control deficits (Karbach et al., 2011; Kray et al., 2008). A behavioural study in the context of TEC by Hommel and colleagues (2011) revealed that processes of event file binding are age-dependent: partial repetition costs, which are reflected by longer RTs and higher error rates in situations when stimulus-response associations are altered across trials, were found to be higher in childhood than in early adulthood, suggesting that the efficiency of updating stimulus-response bindings develop gradually from childhood to adulthood. To date, however, the neural mechanisms underlying the development of event-file coding processes are still largely unclear.

To fill this gap, here we investigated neurophysiological dynamics underlying the development of event file coding using EEG methods. On the basis of event-related potentials (ERP), it was previously possible to detect the temporally segregated stages of information processing during event-file coding in healthy adults and adult patients with Tourette syndrome (Kleimaker et al., 2020; Petruo et al., 2016; Takacs et al., 2020a, 2020b). Furthermore, EEG source localization methods are useful to delineate the underlying functional neuroanatomical networks. For instance, the P1 ERP-component is known to mirror early stimulus categorization and encoding of response-relevant stimuli, specifically in the superior parietal lobe (BA7) (Klimesch, 2011; Petruo et al., 2016), while the P3 ERP-component is associated with processes of selecting the appropriate response in the inferior parietal lobe (BA40) (Petruo et al., 2016; Takacs et al., 2020b). The P3 amplitudes might therefore reflect a reactivation of stimulus-response links and be indicative for event binding. However, it has to be considered that ERPs may not be precise enough to capture different subprocesses of event file coding. That is because different processes from overlapping brain regions are intermingled within the EEG signals and are difficult to discern (Mückschel et al., 2017; Ouyang et al., 2015; Stock et al., 2017; Takacs et al., 2020a, 2020b). Feature binding in the TEC framework encompasses at least three different processes: stimulus-related feature binding into object files, response-related feature binding into action files, and an associative binding that combines both processes into event files (Hommel et al., 2011). In this regard, the residue iteration decomposition method (RIDE) serves to disentangle neurophysiological processes of event file coding. RIDE decomposes the EEG signal into different activity clusters: the S-cluster predominantly related to early sensory attention and perception; the R-cluster related to response preparation and execution of the response; and the C-cluster related to cognitive processes involved in response selection or stimulus-response bindings (Ouyang et al., 2011, 2017, 2015). Given the striking similarities and overlaps of subprocesses involved in event-file coding as proposed by TEC (Hommel et al., 2011), recent studies applying RIDE on data collected using TEC paradigms have found for event file binding processing to be more precisely captured in the C-cluster than in the undecomposed EEG data (Kleimaker et al., 2020; Opitz et al., 2020; Takacs et al., 2020a, 2020b). Of note, the P3 time window is incorporated in the C-cluster. Thus, similar to the P3, results from earlier work showed that the amplitudes of the C-cluster after RIDE decomposition were smaller when feature binding processes were easier and that this was related to better performance (Takacs et al., 2020b). At the source level, these event-coding effects were accompanied by activity changes mainly in the superior frontal gyrus (BA6) and the inferior parietal cortex (BA40).

Earlier and later time ranges, incorporated in the S- and R-clusters, appeared to reflect object- and response-file related processes, respectively (Takacs et al., 2020a, 2020b). RIDE allows to account for intra-individual variability in EEG data (Ouyang et al., 2017). Interestingly, intra-individual performance fluctuations in behaviour and standard ERPs were previously shown to change as a function of age (Bodmer et al., 2018; Li et al., 2004; Papenberg et al., 2013). Such fluctuations during development pose a general challenge when comparing neurophysiological correlates of cognitive performance across age groups. For developmental studies, RIDE has been shown to be a particularly suitable tool to circumvent these comparability problems (Bodmer et al., 2018; Giller et al., 2019). The reason is that RIDE decomposes EEG data into different clusters, based on latency variability. In comparison to standard ERPs, it minimizes residual error due to noise and therefore accounts for individual and age-related differences in intraindividual variability in the data.

In the current study, we investigated event file processing in a large group of healthy participants covering development from late childhood to early adulthood. Our aim was to investigate the development of neural correlates of event file coding. Since it is well conceivable that action control processes may implicate the development of event-file coding and based on previous findings reviewed above, we hypothesized that particularly the C-cluster, but not the S- and R-cluster, would reveal age-related differences of event file processing. Given that the maturation of long-range networks and of the dopaminergic system might affect event file processes (Colzato et al., 2007a, 2007b, 2012, 2013; Colzato and Hommel, 2008; Crone, 2014; Crone and Steinbeis, 2017; Hämmerer et al., 2014; Li, 2012; Luna et al., 2010; Petruo et al., 2016; Takacs et al., 2020b) and that event file processes were differently modulated in relation to age (Hommel et al., 2001), we expected event file processes to develop gradually from childhood into late adolescence. Because the inferior parietal area has been attributed to C-cluster activity modulation during event file processing (Kleimaker et al., 2020; Takacs et al., 2020b) and since parietal regions were associated to maturational processes of cognitive control (Andre et al., 2016; Crone and Richard Ridderinkhof, 2011; Darki and Klingberg, 2015; Luna et al., 2010; Ofen et al., 2012; Shing et al., 2010; van Duijvenvoorde et al., 2016), we further hypothesized that parietal regions **may underlie age-related differences** during event file coding.

2. Methods

2.1. Participants

A sample of N = 91 participants in the age range from 10–30 years was recruited (44 females and 47 males, mean age = 18.14, SD = 6.23, 74 right-handed). Among the participants, there were n = 54 children and adolescents under the age of 18 (29 females) and n = 37 adults above the age of 18 (15 females). Handedness was assessed through self-report and during the interview and was unknown for 11 participants. As confirmed by clinical interviews and questionnaires, they did not report any history of psychiatric or neurological disorders, did not take centrally acting medication, and had normal or corrected-to-normal vision. Children and adults were recruited from participant pools of the Technische Universität Dresden, the University Clinic Carl Gustav Carus, the Universität zu Lübeck, and the Eötvös Loránd University in Hungary. Across all study sites, each subject received financial compensation of 50€ after participating in this experiment.

Prior to the experimental procedure, all participants were informed about the procedures for data collection and publication. Written consent was provided by all subjects or their legal guardians (in case of children) prior to study participation. The study was performed in accordance with the declaration of Helsinki and was approved by the ethics committee of the TU Dresden (EK 359092017).

2.2. Task

The present study used the "automatic" event file coding paradigm (Hommel, 1998; Hommel et al., 2001), which has been slightly modified and used in our group before (Colzato et al., 2006; Kleimaker et al., 2020; Petruo et al., 2016, 2016; Takacs et al., 2020a, 2020b). A schematic diagram of the paradigm is shown in Fig. 1.

Participants performed the task on a 17-inch CRT screen, at a distance of 60 cm. Three vertically aligned boxes, each measuring 2.4 × 0.9 cm, were presented in the middle of the screen. First, a response cue was presented in the middle box, which was either a left- or right-pointing arrowhead. The cue orientation needed to be remembered and was relevant for the first response execution (R1). After the presentation of the cue, two vertically or horizontally aligned lines corresponding to Stimulus 1 (S1) and by the following Stimulus 2 (S2) appeared. S1 and S2 varied randomly in orientation (vertical or horizontal), location (top or bottom), and colour (red or green). Thus, trials differed in the amount of feature overlaps between S1 and S2: no feature overlap, partial (one or two) feature overlap, or full (identical) feature overlap. In every trial, response R1 and response R2 had to be carried out following the stimuli (S1 or S2, respectively). To respond, participants used the left index finger to press the left key, or the right index finger to press the right control key of a computer keyboard. Thus, R1 and R2 within a trial could be identical in response repetition condition or different in the response alternation condition. Participants were told that S1 and S2, and S1 and R1 were not systematically related to each other. R1 was entirely independent of the orientation, colour, or location of S1, but due to their temporal proximity, stimulus features of S1 can be cognitively bound to R1. Regarding the timing of each trial, the cue was first presented for 1500 ms, followed by a blank screen (1000 ms). Participants were instructed to carry out the first response (R1) (i.e. right or left keypress) according to the direction shown by the cue (right- or left-pointing arrowhead) after S1 appeared (presentation duration: 500 ms). Subsequently, a blank screen (2000 ms) was followed by S2, which lasted 2000 ms or until R2 was executed. R2 was the response to the orientation of S2 (i.e. a left keypress was required when a lying rectangle and a right key when a standing rectangle was shown). The whole session included at least 384 trials, which were divided into three blocks of 128 trials. In case R1 was incorrect, the same trial was repeated three times at maximum. The current sample did not exceed the presentation of 597 trials ($M = 444.7$; $SD = 45.3$). Between trials, a fixation cross was shown in the middle of a black screen (1500–2000 ms).

The common finding using this task is that previously established event file bindings, which are due to identical stimuli require different responses (as in the response alteration condition, cause problems because expectancies on stimulus-response associations are not or only partially fulfilled under such circumstance. This requires reconfiguration of the event file and integrated sensorimotor associations, which could slow down responses and increase error rates. In contrast, responding is facilitated whenever identical/similar stimuli trigger the same responses. Therefore, binding is reflected by an interaction "feature overlap x response". The binding effect was defined as the difference values of full feature overlap minus the no feature overlap condition for each of the two response conditions (alteration vs. repetition). As a first step, we checked whether the principal task effects associated with the event-file coding paradigm are also observed in our sample covering a broad age range. Results presented in sections 3.1.1,3**.1.2 and 3.2 report task effects for the accuracy and reaction time, and neurophysiological data, respectively. In the second step, we conducted correlational analyses to investigate age-related effects and the results are reported in** sections 3.1.3 **(behavior effects) and 3.3 (neurophysiological effects).**

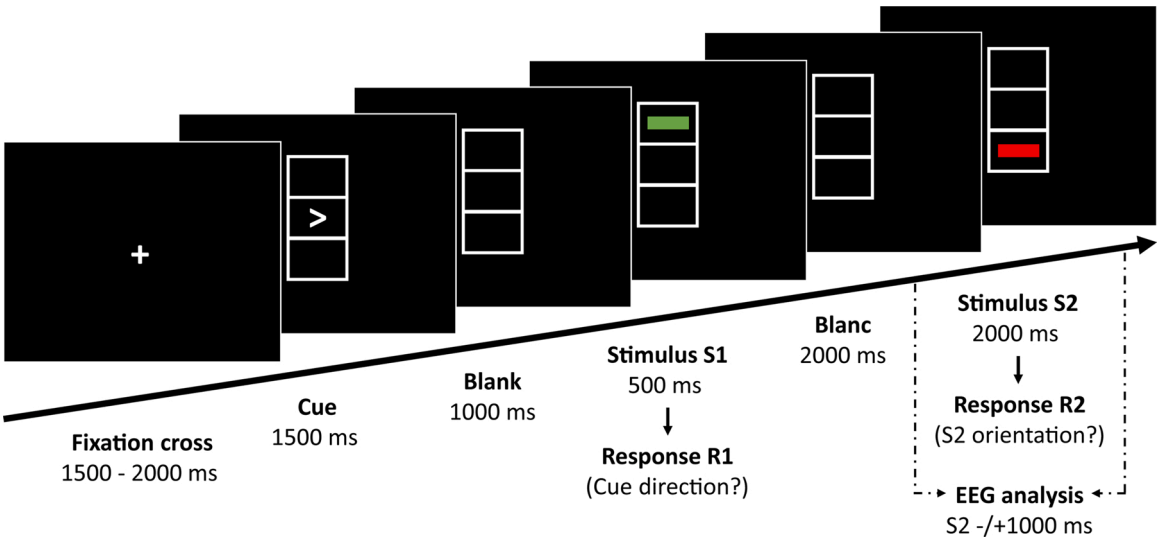

Fig. 1. Schematic illustration of the task. In each trial, participants were first asked to look at a fixation cross prior to cue and stimulus presentation. After S1, participants responded depending on cue direction (R1). Following S2, participants answered in relation to the shape (an upright, standing rectangle or a lying, horizontal rectangle) of S2 (R2). Each stimulus varied randomly in orientation (vertical or horizontal), location (top or bottom), and colour (red or green).

2.3. EEG recording and processing

To record the EEG, 60 Ag/AgCl electrodes (EasyCap, Germany) were connected to a BrainAmp amplifier and to the Brain Vision Recorder 1.2 software (Brain Products, Germany). The cap layout is based on the standard 10 %-system but with equidistant electrode positions. The coordinates for the ground electrode were at $\theta = 58$, $\varphi = 78$ and for the reference electrode at $\theta = 90$, $\varphi = 90$. The sampling rate was 500 Hz, and all electrode impedances were kept below 5 kΩ. Data pre-processing steps were performed using Brain Vision Analyzer II (Brain Products) and corresponded to the previous studies of our lab analysing event coding data (Kleimaker et al., 2020; Takacs et al., 2020a, 2020b). The EEG data were down-sampled to 256 Hz, band-pass filtered (IIR filter: 0.5–20 Hz, order of 8), and then re-referenced to an average reference. Technical artifacts were removed with a manual inspection of the data. **That is, the data were screened by an examiner and periods in the data relating to breaks between the three task blocks were discarded. Moreover, the data were screened for gross technical artifacts (e.g., offsets in the EEG) and these parts of the data were also discarded.** The independent component analysis (Infomax algorithm) was used to eliminate remaining periodical artifacts, such as eye movements, cardiovascular or muscular activity. Next, segmentation was performed resulting in epochs of −1000 ms before S2 presentation until 1000 ms after S2. Although event file binding occurs after the creation of S1-R1-links, retrieval, unbinding, and updating processes are typically studied after S2-R2 establishment (Hommel, 1998). The analysis only comprises trials with correct R1 and R2 responses. For all combinations of the four feature overlap levels (no, one, two, and full overlap between S1 and S2) and for the two response types (repetition vs. alternation) separate segments were created. **An automated artifact rejection procedure in the segmented data was conducted in the time period spanning an interval starting 1000 ms before and ending 1000 ms after the S2. The criteria were as follows:** segments containing amplitudes higher than 150 μV, lower than −150 μV or activities lower than 0.5 μV over a time interval of at least 100 ms were discarded. A current source density (CSD) transformation was applied (Kayser and Tenke, 2015) to gain reference-free EEG data. A baseline correction was performed on a time interval of −200 to 0 ms prior to the S2 stimulus onset. Finally, data of each experimental condition (overlap level and response type) and each participant were averaged.

2.4. Residue iteration decomposition

After the initial pre-processing steps, the EEG data was further processed using the residue iteration decomposition (RIDE) (Ouyang et al., 2015, 2011). RIDE allows to account for intra-individual variability, but also to distinguish different event file processing stages that are intermixed in usual ERPs (Mückschel et al., 2017, 2017; Ouyang et al., 2015; Takacs et al., 2020a, 2020b). Based on latency variability of different components, which correspond to different information processing levels, RIDE decomposition is employed on single-trial ERPs and separately for each electrode. The current study applied RIDE according to established procedures (Kleimaker et al., 2020; Mückschel et al., 2017; Ouyang et al., 2015; Takacs et al., 2020a, 2020b) in MATLAB (MathWorks, Inc., Natick, MA) and based on the RIDE toolbox (for a manual, see http://cns.hkbu.edu.hk/RIDE.htm). By estimating latency information from stimulus and response onsets, we obtained the S ("stimulus") and R ("response") clusters. The C ("central") clusters are extracted by estimating and iteratively improving the latency information in every single trial. Time windows for each cluster are predefined such that the S-cluster covers the stimulus onset and the following processes from P1 to N2, the R-cluster occurs around the response, and the C-cluster incorporates the time ranges of P2, N2, and P3 (Ouyang et al., 2017, 2015). Accordingly, we applied the interval from 200 ms prior to S2 presentation to 700 ms after S2 for the S-cluster; from 300 ms before until after R2 for the R-cluster and from 150 ms to 800 ms after S2 for the C-cluster. An iterative decomposition with an *L1*-norm minimization is used in RIDE, which generates median waveforms. That is, C and R are subtracted from each trial and the residual of all trials are aligned to the latency information of S. Consequently, the median waveform in the S-cluster interval are obtained for all time points. Therefore, RIDE-decomposed data is less prone to intra-individual variability in the data in contrast to standard ERP, which is rather based on simple averaging and minimization of the *L2*-norm of the data (Ouyang et al., 2015, 2011). To estimate the C- and R-clusters, the same procedure is performed. Please refer to Ouyang et al. (Ouyang et al., 2015) for further detailed descriptions of the RIDE procedure. For data quantification, we selected electrodes based on scalp topography plots and determined the corresponding time windows by visual inspection. Results from our sample spanning a wide age range showed that amplitude latencies and related electrode sites differ between children and adults. We therefore selected new time windows and considered new electrodes incorporating latency information of the whole developmental sample and

which cannot lean on previous methodologies that included adult samples only (Takacs et al., 2020b, 2020a). The S-cluster was selected at electrode P7, based on scalp topography. After visual inspection, we chose the time range of 80–150 ms in order to obtain P1 component information, and the time range between 150–210 ms to obtain the N1. For comparability, we also analysed electrode P8 at the contralateral side, using the same time intervals. For the C-cluster, we chose the P3 time window because this was found to reflect event-file coding in previous studies (Petruo et al., 2016; Takacs et al., 2020b). We pooled the C-cluster data across electrodes P3, PO1 and P7, because the positive peak (i.e. P3 component) was most pronounced across these electrode sites and we selected the time range of 300–600 ms. To assess event-file coding in the R-cluster, we selected electrode P4, because this electrode revealed the strongest P3 component signal in the time between 400–500 ms. Because we were interested in potential processes in the motor cortex, we additionally selected the electrodes C3 and C4 within the same R-cluster time range. Finally, the mean amplitudes for the corresponding time intervals were extracted at the single-subject level.

2.5. Source localization

We used sLORETA (standardized low-resolution brain electromagnetic tomography) (Pascual-Marqui, 2002) to examine which functional neuroanatomical structures are linked to RIDE-decomposed EEG activity correlating with age. sLORETA provides a single linear solution to the inverse problem without a localization bias (Marco-Pallarés et al., 2005; Pascual-Marqui, 2002; Sekihara et al., 2005).The validity of the approach has been corroborated by TMS and EEG/fMRI studies (Dippel and Beste, 2015; Ocklenburg et al., 2018; Sekihara et al., 2005). sLORETA uses the MNI152 template (Mazziotta et al., 2001) and the intra-cerebral volume is split in voxels with 5 mm spatial resolution. For each voxel, the current density is calculated using a realistic head model (Fuchs et al., 2002). sLORETA was calculated for time period in the EEG data correlating with age **(see** section 3.3 **in the results)**. **In a data-driven analysis step, we examined which time period after the locking time point (i.e. time point zero; S2 stimulus presentation) revealed significant correlations between RIDE-decomposed EEG-amplitude data and age.** For time periods correlating with age (see results section for details), **the mean source of** the EEG activity in this time period was estimated. Statistically, this refers to contrast against zero. This contrast was computed using the sLORETA-built-in voxel-wise randomization tests with 2000 permutations, based on statistical non-parametric mapping (SnPM). Significant voxels with significant differences ($p < .01$, corrected for multiple comparisons) were shown in the MNI-brain.

2.6. Statistics

For statistical analyses, SPSS (IBM Corp. Released 2017) was used. For the behavioural data, mean accuracy (percentage of correct responses) and mean RTs (for correct responses) of each participant and each experimental condition were computed. Regarding effects of feature overlap, the accuracy and RT data were analysed in two-way repeated measures analysis of variance (ANOVA) with the number of overlapping features (no, one, two, and full overlap between S1 and S2 features) and response (repetition vs. alternation) as within-subject factors. This was done to examine the principle findings of event file binding effects observed in previous studies (Colzato et al., 2006; Hommel et al., 2001; Kleimaker et al., 2020; Petruo et al., 2016; Takacs et al., 2020a, 2020b). This analysis confirmed that the strongest effects of response alternation vs. response repetition were evident between the no feature and the full feature overlap conditions (see results section). Similar to previous studies, we therefore only used these two feature overlap conditions for the binding effect analysis (Beste et al., 2016; Kleimaker et al., 2020; Takacs et al., 2020a, 2020b). The binding effect was defined as the difference values of full feature overlap minus the no feature overlap condition for each of the two response conditions (alteration vs. repetition). Higher values indicate stronger binding effects, irrespective of whether there were partial repetition benefits or costs. To examine developmental effects on event file processing, a hierarchical multiple regression analysis with four steps were performed either with respect to RT or the accuracy data, in order to evaluate the relation between age and the effect of feature overlap (computed as the difference score between the full and no-overlap conditions) and of age. For the RIDE-decomposed EEG data, ANOVAs were used including the within-subject factors feature overlap (no feature overlap and full feature overlap) and response (repetition vs. alternation). The following average number of trials (with the minimum and maximum numbers) were entered in the EEG analysis: no feature overlap repetition M = 17.4, (7–28); no feature overlap alternation M = 20.8, (8–29); full overlap repetition M = 20.9, (5–33); full overlap alternation M = 18.3, (6–30). Similar numbers were found for previous studies on event file coding (Petruo et al., 2016; Takacs et al., 2020b). As mentioned before, RIDE uses the *L1*-norm minimization method, which accounts for intra-individual variability and therefore allows to obtain more reliable effects with low trial numbers compared to standard ERP approaches (Ouyang et al., 2015, 2011). In the S- and R-cluster, electrode positions were included as within-subject factor (P7 and P4; C3 and C4, respectively). We reported η^2_p effect sizes for the ANOVA. Bonferroni correction was performed on all pairwise comparisons.

3. Results

3.1. Behavioral data

The accuracy and RT data based on the entire sample are shown in Fig. 2.

3.1.1. Accuracy

The ANOVA for the accuracy data showed the following results: A significant main effect for the response condition was found ($F(1,90)$ = 17.1, $p < 0.001$, $\eta^2_p = 0.160$), with participants showing lower scores in the response repetition condition than in the alternation condition (84.86 % ± 1.10 vs. 88.24 ± 0.93). No main effect was found for feature overlap ($F(3,90) = 1.42$, $p = 0.24$, $\eta^2_p = 0.016$). Crucially, as anticipated, the feature overlap x response interaction was significant ($F(3,90)$ = 104.7, $p < 0.001$, $\eta^2_p = 0.538$), indicating that there was a binding effect: When the repetition of the response was required, accuracy scores increased from the no feature overlap (78.04 % ± 1.57) to the one feature overlap (83.08 % ± 1.23, $p < 0.001$), the two features overlap (86.54 % ± 1.23, $p < 0.001$) and the full feature overlap condition (91.69 % ± 0.88, $p < 0.001$). In contrast, in cases where alternation of the response was required, accuracy scores decreased from the no feature overlap (93.60 % ± 0.82) to the one feature overlap (91.05 % ± 0.83, $p = 0.001$), the two feature overlap (86.33 % ± 1.18, $p < 0.001$) and the full feature overlap condition (81.98 % ± 1.48, $p < 0.001$). The remaining pairwise comparisons were also significant (all $p < 0.001$).

3.1.2. Reaction time

Regarding the RT data, a significant main effect for feature overlap was found ($F(3,90) = 6.23$, $p = 0.002$, $\eta^2_p = 0.065$), with faster RTs in the no feature overlap condition (542 ms ± 14), than in the one feature (555 ms ± 14, $p = 0.003$), the two feature (556 ms ± 14, $p = 0.002$) and the full feature overlap condition (557 ms ± 15, $p = 0.036$). Other pairwise comparisons were not significant (all $p > 0.05$). A significant main effect was also found for response type ($F(1,90) = 5.33$, $p = 0.023$, $\eta^2_p = 0.056$), indicating faster RTs for the response alternation condition (549 ms ± 14), compared to the response repetition condition (556 ms ± 14). Importantly, a significant feature overlap x response interaction was found ($F(1,90)$ = 45.6, $p < 0.001$, η^2_p = 0.336), which reflects binding. Specifically, when repetition of response was required, RTs were faster in the full feature overlap condition (542 ms ± 14),

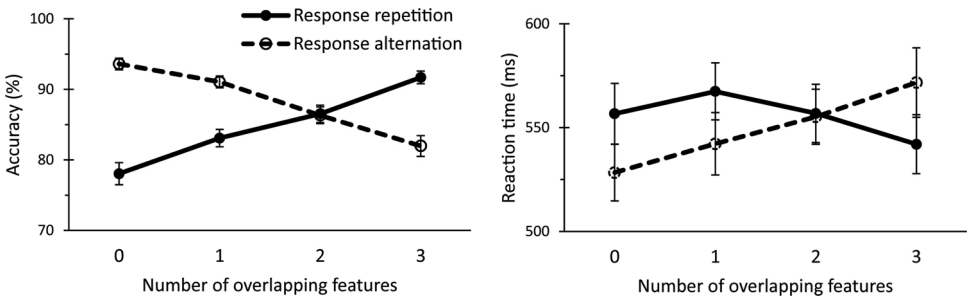

Fig. 2. Mean accuracy and mean RT across overlapping feature levels for repeated (black line) and alternated (dashed line) responses based on the entire sample. Error bars represent standard error of mean.

compared to the two features overlap (557 ms ± 14, $p = 0.006$), the one feature overlap (567 ms ± 15, $p < 0.001$) and the no feature overlap condition (557 ms ± 15, $p = 0.026$). Additionally, the reaction time in the one feature overlap condition was slower than in the two features overlap condition ($p = 0.034$). Alternation of responses, on the contrary, lead to faster RTs when no feature overlapped (528 ms ± 14) than when one feature overlapped (542 ms ± 14, $p = 0.020$), when two features overlapped (555 ms ± 13, $p < 0.001$) and when all features overlapped (572 ms ± 17, $p < 0.001$). RTs in the one feature condition were also faster compared to both the two feature and full feature overlap condition ($p < 0.001$). The other pairwise comparisons were not significant (all $p > 0.05$).

3.1.3. Age-related effects

In our age continuous sample, we analysed age-related effects by conducting hierarchical multiple regression analyses separately for the accuracy and RT data. Since we were particularly interested in the development of binding, we first computed difference scores between full feature overlap and no feature overlap for each of the two response conditions (alternation vs. repetition). This was done because contrasting these conditions reveals the strongest binding effects in accuracy and RT. The hierarchical regression analysis includes four steps, with age as the dependent variable. Accuracy or RT difference score derived from the response alternation condition was entered as a predictor in the first step, followed by difference score from the response repetition condition, the interaction between the scores of the two conditions and gender as predictors in the second, third and fourth step, respectively.

Results regarding the accuracy data showed that difference score from the alternation condition did not significantly predict age differences ($\beta = 0.22$, $t = 1.36$, $p = 0.18$), whereas difference score from the repetition condition did significantly predict age differences ($\beta = -0.44$, $t = -2.96$, $p = 0.04$). The interaction between effects of feature overlap in the alternation and repetition conditions also significantly predicted age differences ($\beta = -0.48$, $t = -2.34$, $p = 0.021$). Gender did not significantly predict age differences ($\beta = -1.12$, $t = -1.12$, $p = 0.27$). In contrast, results concerning the RT data did not reveal any significant relations with age, neither for RT difference score derived from the alternation condition ($\beta = -0.20$, $t = -1.74$, $p = 0.09$), nor from the repetition condition ($\beta = 0.11$, $t = 0.75$, $p = 0.46$), their interaction ($\beta = -0.089$, $t = -0.64$, $p = 0.53$) or gender ($\beta = -0.063$, $t = -0.58$, $p = 0.56$). Taken together, these results show that age-related developmental difference in the effect of feature overlap on stimulus-response binding was only observed in performance accuracy but was not present in the RT data. Furthermore, the age-related effect depends on whether the responses had to be repeated or alternated. With increasing age, the partial repetition benefit of repeating the responses decreases, which suggests a gradual development of lesser reliance on processes that are associated with executing motor actions for event coding. Although response alternation (switching) resulted in partial repetition cost in terms of reducing performance accuracy (see Fig. 2), this cost was of similar extent for individuals of different ages.

3.2. Neurophysiology data (principal task-related effects)

For EEG analysis, only difference scores between full and no feature overlap were used. **The analyses reported in this section are only presented to examine that general task effects reported in the literature are evident in this data set as well. The main focus is the analysis on age-related correlations presented in** section 3.3 (Fig. 3).

As mentioned before, contrasting these two conditions shows the strongest binding effects. For the S-cluster, the ANOVA showed a main effect for electrode position when analysing the P1 time range ($F(1,90) = 15.9$, $p < 0.001$, $\eta^2_p = 0.150$). Mean amplitudes were higher at electrode P8 (12.1 $\mu V/m^2 \pm 1.2$) compared to electrode P7 (7.53 $\mu V/m^2 \pm 1.21$). No significant main effect was found for feature overlap ($F(1,90) = 1.52$, $p = 0.221$, $\eta^2_p = 0.017$) or for response type, ($F(1,90) = 0.47$, $p = 0.493$, $\eta^2_p = 0.005$). The electrode x feature overlap, electrode x response, feature overlap x response, as well as the three-way electrode x feature overlap x response interactions did not reveal significant effects (all $F < 4.00$, $p > 0.05$). In the N1 time range, results of the S-cluster showed a significant main effect for electrode position ($F(1,90) = 11.9$, $p = 0.001$, $\eta^2_p = 0.117$), with higher negative values for P7 (-8.31 $\mu V/m^2 \pm 1.90$), compared to P8 (-1.70 $\mu V/m^2 \pm 2.32$). There was no main effect for feature overlap ($F(1,90) = 2.16$, $p = 0.145$, $\eta^2_p = 0.023$) or for the response condition ($F(1,90) = 0.46$, $p = 0.500$, $\eta^2_p = 0.005$). There were also no interactions for electrode x feature overlap, electrode x response and feature overlap x response interaction (all $F < 4.00$, $p > 0.05$). However, the feature overlap x response x electrode interaction was significant ($F(1,90) = 4.53$, $p = 0.036$, $\eta^2_p = 0.048$). However, follow-up analyses were not significant for P7 ($F(1,90) = 3.04$, $p = 0.085$, $\eta^2_p = 0.033$) or P8 ($F(1,90) = 0.677$, $p = 0.413$, $\eta^2_p = 0.007$). Grand-average waveforms on P7 and P8 for the S-cluster are shown in Fig. 4.

Grand-average waveforms within the P3 time window for the C-cluster are shown in Fig. 5. **The scalp topography plot (see Fig. 5) revealed activity in the P3 time window that was spread over posterior electrode sites with a slight left-ward accentuation in the no feature overlap condition, in which responses were repeated. Inspection of the data revealed that amplitudes were highest at the electrode sites P3, PO1 and P7, which were thus pooled for the data analysis. The** ANOVA showed a main effect of feature overlap ($F(1,90) = 8.69$, $p = 0.004$, $\eta^2_p = 0.088$), with larger mean amplitudes in the no feature overlap condition (13.4 $\mu V/m^2 \pm 1.05$) than in the full feature overlap condition (9.14 $\mu V/m^2 \pm 0.98$). No main effect for response type was found ($F(1,90) = 2.68$, $p = 0.105$, $\eta^2_p = 0.029$). The interaction feature overlap x response was significant ($F(1,90) = 5.66$, $p = 0.019$, $\eta^2_p = 0.059$). Specifically, mean amplitudes dropped from the no feature overlap to the full feature overlap condition in cases where responses repeated (15.3 $\mu V/m^2 \pm 1.38$ vs. 8.82 $\mu V/m^2 \pm 1.20$, $p = 0.001$, $d = 0.523$). Mean amplitudes also dropped from the no feature overlap to the full feature overlap condition in response alternation conditions, but this was not significant (11.5 $\mu V/m^2 \pm 1.13$ vs. 9.50 $\mu V/m^2 \pm 1.12$, $p = 0.174$, $d = 0.195$).

The scalp topography plots of the R-cluster revealed that

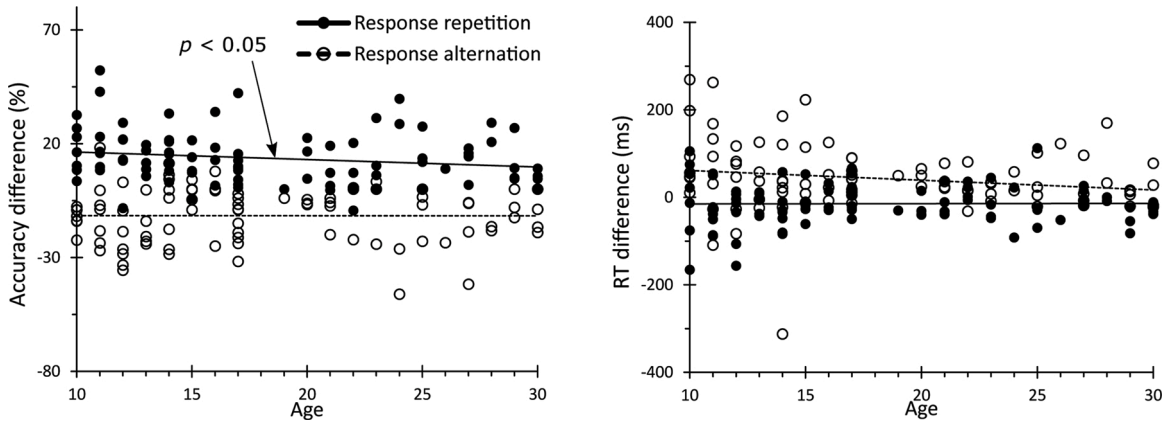

Fig. 3. Correlation between accuracy score and mean RT differences (i.e. full feature overlap minus no feature overlap) and age. Correlations are depicted for both the response repetition (black line) and the alternation condition (dashed line).

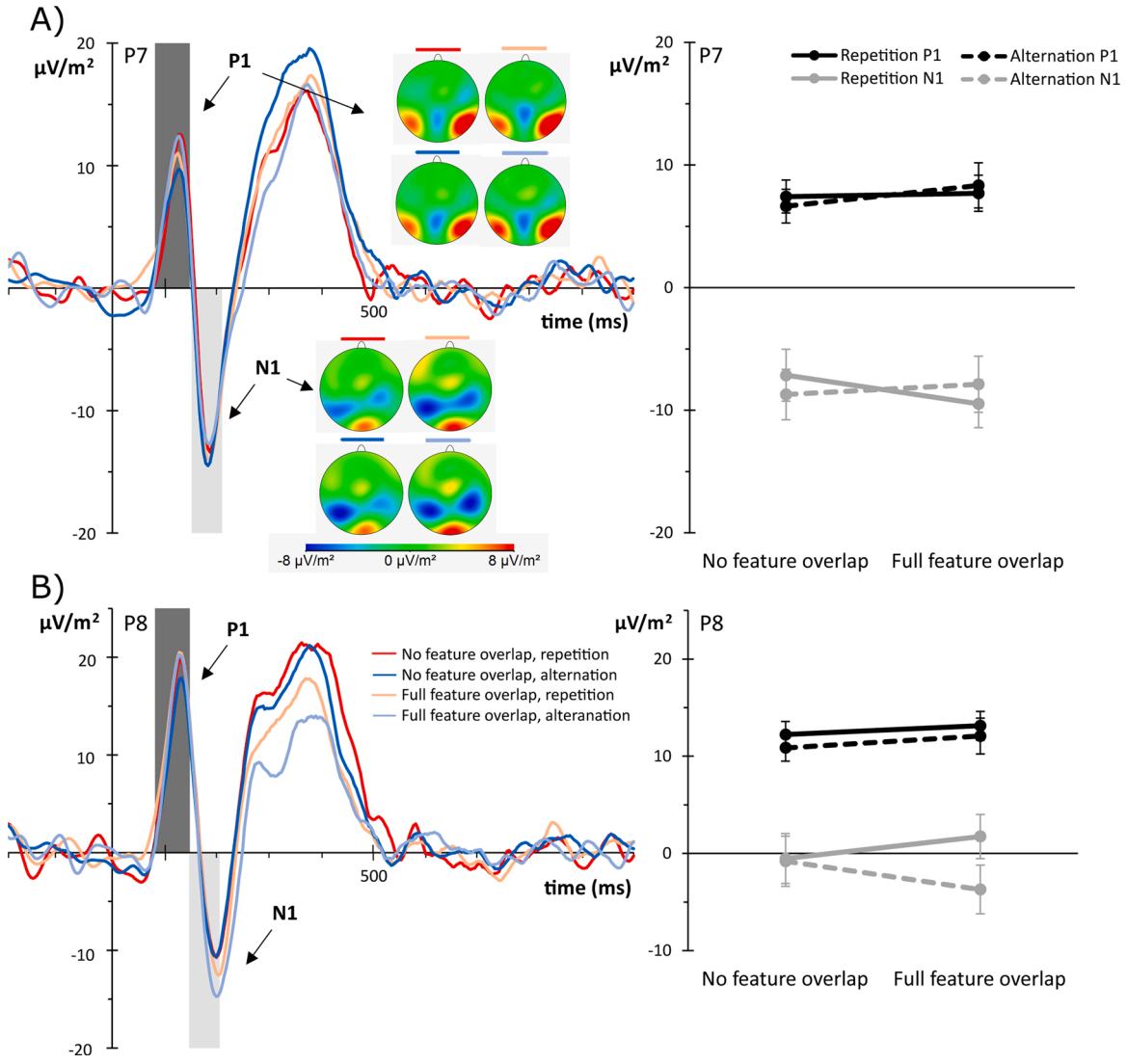

Fig. 4. Mean amplitude activity of the S-cluster in the P1 (80-150 ms, black shaded area) and N1 (150-210 ms, grey shaded area) time window for the P7 electrode (A) and the P8 electrode (B). S2 is presented at timepoint zero. Scalp topography plots depict the mean activity distribution in the respective time window across the four conditions. The line graphs show mean amplitudes for the feature overlap x response interactions, for the P1 time window (black lines) and N1 time window (grey lines), with standard errors.

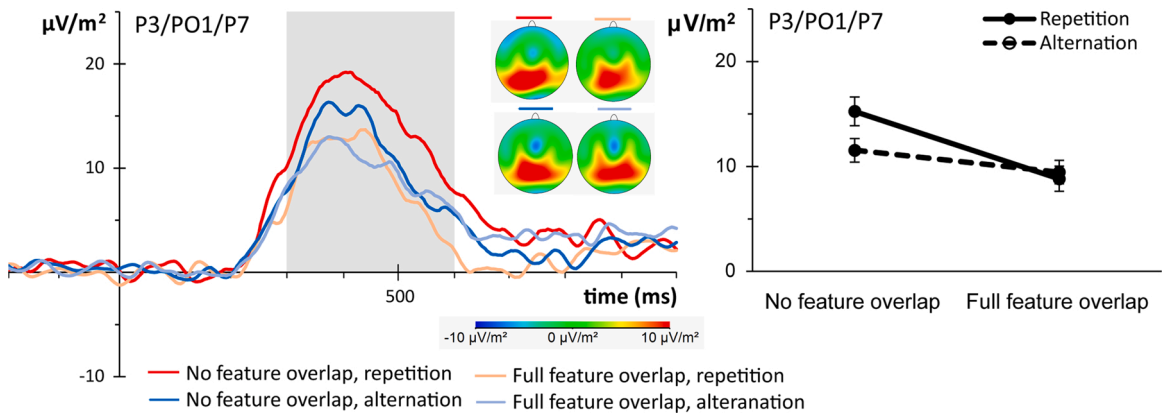

Fig. 5. Mean amplitude activity in the P3 time window for the C-cluster (300-600 ms). S2 is presented at timepoint zero. The analysed time window is in shaded grey. Scalp topography plots illustrate the mean activity distribution in the respective time window across each of the experimental conditions. The line graph shows mean amplitudes for the feature overlap x response interactions, with standard errors.

activity was not only evident at central (motor) regions (which can be captured by C3 and C4 electrodes), but also revealed activity at posterior electrode leads. Analyzing the R-cluster at electrode P4 (Fig. 6A**), the** ANOVA showed no main effect for feature overlap ($F(1,90) = 0.009$, $p = 0.926$, $\eta^2_p < 0.001$), and no main effect for response type ($F(1,90) = 0.35$, $p = 0.554$, $\eta^2_p = 0.004$). The feature overlap x response type interaction revealed significant results ($F(1,90) = 4.63$, $p = 0.034$, $\eta^2_p = 0.049$). When the response was repeated, mean amplitudes were larger for full overlapping features than for the no overlapping features condition (7.82 µV/m² ± 1.17 vs 5.99 µV/m² ± 1.28, $p = 0.103$, $d = 0.156$). When the response was alternated, mean amplitudes were lower when all features overlapped than when no features overlapped (5.12 µV/m² ± 1.17 vs 7.13 µV/m² ± 1.21, $p = 0.201$, $d = -0.177$).

Since the R-cluster reflects activity related to the motor response, we also examined the R-cluster at electrode C3 and C4, which overlie the motor cortex (Fig. 6B and C). Results revealed a significant main effect for feature overlap ($F(1,90) = 5.35$, $p = 0.023$, $\eta^2_p = 0.056$). The no feature overlap condition showed higher amplitudes than the full feature condition (2.12 µV/m² ± 0.69 vs. 0.32 µV/m² ± 0.86). The main effect for response condition was significant ($F(1,90) = 7.56$, $p = 0.073$, $\eta^2_p = 0.077$) with higher amplitudes in the repetition condition compared to the alternation condition (2.32 µV/m² ± 0.77 vs. 0.11 µV/m² ± 0.80). No main effect was found for channel position ($F(1,90) = 3.33$, $p = 0.071$, $\eta^2_p = 0.036$). No effects were found for all types of interactions, which are electrode x feature overlap, electrode x response, feature overlap x response, as well as feature overlap x response x electrode (all $F < 4.00$, $p > 0.05$).

Taken together, the neurophysiological data pattern well replicates general findings on task-related effects (i.e. effects of the experimental manipulations) found in other studies (Kleimaker et al., 2020; Petruo et al., 2016; Takacs et al., 2020b). This validates the methodological approach taken for the EEG data analysis.

3.3. Neurophysiological data (age-related effects)

To investigate developmental effects in event file binding at a neurophysiological level, we correlated the RIDE-decomposed EEG data with age. In order to find the relevant electrodes and the specific time intervals to explore developmental effects we used a completely data-driven approach where age was correlated with the amplitudes for every time point at each electrode. **This was done because there were no clear a-priori hypotheses could be derived based on existing literature to inform at which electrode and time window possible correlations of neurophysiological processes with age are most evident. To this end, and in line with the procedure taken in the analysis of the** behavioural data, the difference of the amplitudes in the full overlapping features minus the no overlapping feature condition for each response condition (alternation and repetition) was calculated and analysed separately for each RIDE cluster. Given that this study only detected event file binding effects (i.e. significant feature overlap x response interactions) in the C- and R-cluster, we excluded any age-related analysis on the S-cluster. Although the regression model showed a significant contribution of only the response repetition condition for accuracy data, both response conditions (including alternation) were tested for potential effects at the neurophysiological level. We analysed both conditions, because underlying mechanisms of binding effects might manifest differently at the neurophysiological level than through behavioural measures such as accuracy and RT. Each data point within a time range of – 200–1000 ms and of each electrode was then correlated with age. This procedure was performed by controlling for the False Discovery Rate (FDR) per electrode, according to Benjamin & Hochberg (1995). Based on this method, we identified the electrodes and time intervals which best reflected the significant correlations of EEG activity and age. This method was performed for each cluster separately (Fig. 7A and B). Scatterplots of the obtained correlations at the corresponding electrodes and time windows are shown in Supplementary Fig. 1. In the C-cluster, correlation analysis revealed that the mean amplitude difference between the feature overlap conditions in the alternation condition correlated negatively with age at electrode FC4 in the time period of 260 ms–340 ms after S2 presentation ($r = -0.39$, $p < 0.05$). In the repetition condition, a negative correlation was found at electrode FC2 in the time period of 250–380 ms ($r = -0.39$, $p < 0.05$). Using these time periods for further sLORETA analysis revealed that the correlations were associated with activation modulations in the superior parietal cortex for both the alternation condition (BA7; MNI [x,y,z]: -6,-53,70) and the repetition condition (BA7; MNI [x,y,z]: -10,-65,65). Correlation on the R-cluster showed a positive correlation only in the alternation condition at electrodes P8 ($r = 0.36$, $p < 0.05$) and P10 ($r = 0.37$, $p < 0.05$) and at the time period of 438–460 ms. sLORETA indicated that the activity was modulated in the superior parietal cortex (BA7; MNI [x,y,z]: -5,-65,65).

4. Discussion

This study's aim was to further characterize processes of feature binding and response selection in the context of TEC by providing a more profound understanding of the neurophysiological correlates accompanying the development of these mechanisms from late childhood to early adulthood. **Mechanisms underlying processes of binding stimulus and response features are of central importance in the context of developmental cognitive neuroscience, because**

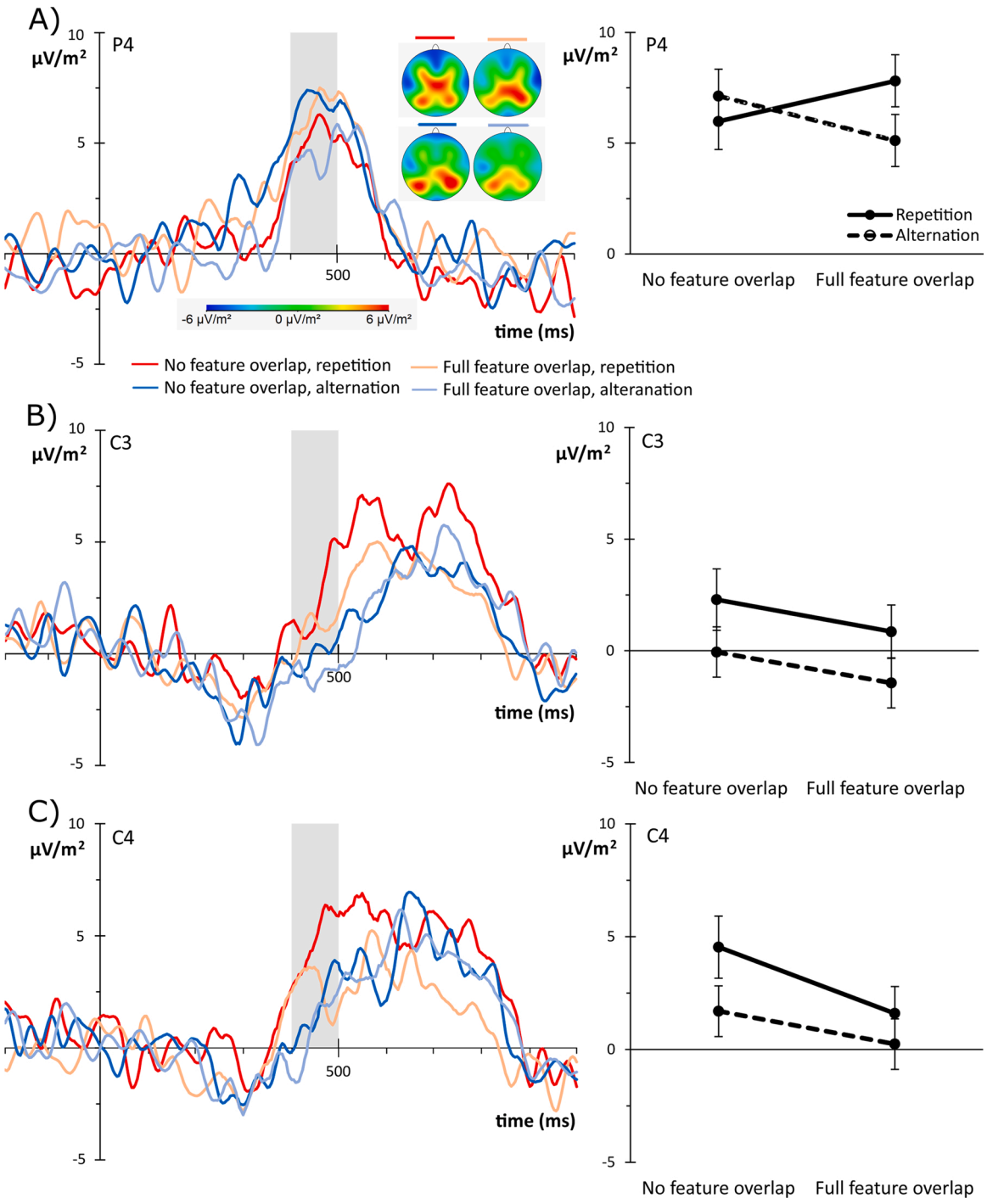

Fig. 6. Mean amplitude activity in the P3 time window for the R-cluster (400-500 ms) at electrode P4 (A), C3 (B) and C4 (C). S2 is presented at timepoint zero. The analysed time windows are marked with a shaded area. Scalp topography plots show the mean activity distribution in the respective time window across the four conditions. The line graphs show mean amplitudes for the feature overlap x response interactions, with standard errors.

cognitive control processes are subject to strong developmental changes across childhood and young adulthood (Friedman et al., 2009; Luna, 2009; Luna et al., 2010; Marek et al., 2015; Munakata et al., 2012; Vedechkina and Borgonovi, 2021) **and a common theme that runs through all these lines of research in cognitive control is how stimulus input becomes associated with a particular response and how this association becomes represented** (Freund et al., 2021)**. The TEC framework represents one important theoretical framework addressing this.** Both at the behavioural and the neurophysiological level, the results of this study revealed event file binding effects (Hommel et al., 2001) and shed new light on age-related differences in processes of event file coding.

On the behavioural level, our results confirm previous well-established findings on event file bindings (Colzato et al., 2006; Hommel et al., 2001; Hommel, 2009; Hommel et al., 2011; Kleimaker et al., 2020; Petruo et al., 2016; Takacs et al., 2020a, 2020b); i.e. that there was an interaction of feature overlap x response, reflecting partial repetition benefits and costs and event file binding (Colzato et al., 2006; Hommel, 1998; Hommel et al., 2001). More importantly, the strength of binding (i.e. the difference between the full feature overlap and the no

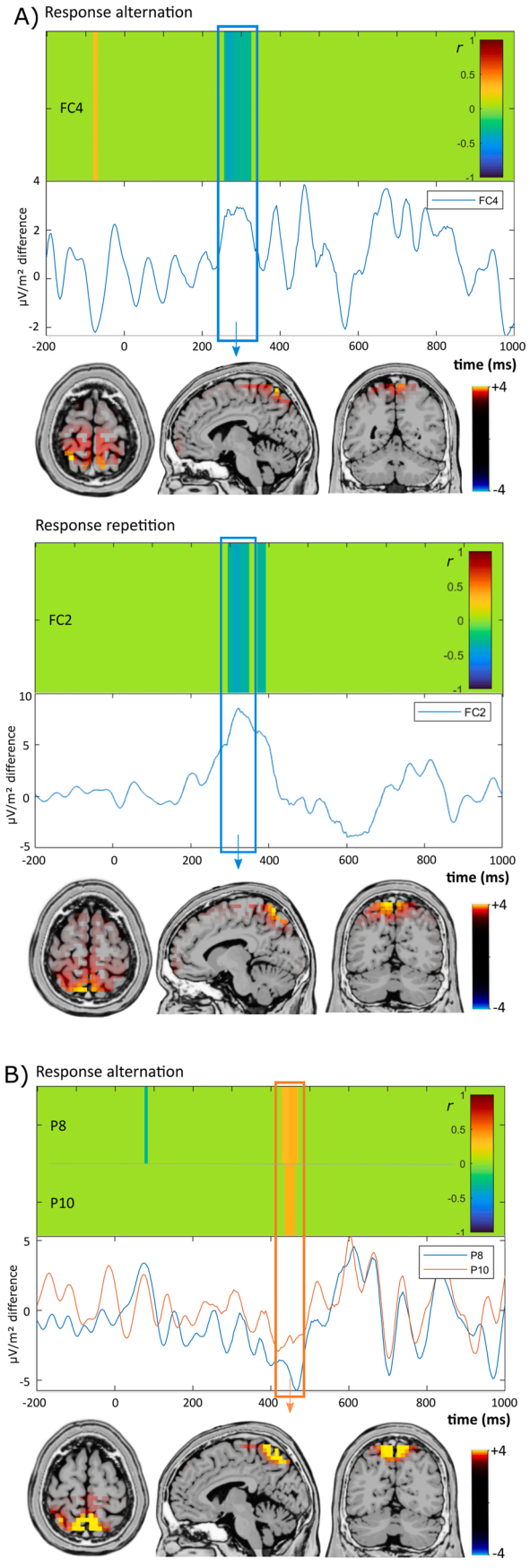

(caption on next column)

Fig. 7. Correlations between RIDE-decomposed EEG data and age, based on mean amplitude differences between the full feature and no feature overlap (full–no) conditions. A) C-cluster: negative correlation at electrode FC4 within the alternation condition (top), 260-340 ms after S2 presentation and at electrode FC2 within the repetition condition (below), 250-380 ms after S2 presentation. sLORETA showed correlation modulation in the superior parietal cortex (BA7) in both conditions. B) Positive correlation in the alternation condition in the R-cluster at electrodes P8 and P10, 438-460 ms after S2 presentation. sLORETA indicated activity modulation in the superior parietal cortex (BA7).

feature overlap) linearly decreased as a function of increasing age, which was the case for accuracy scores in the repetition condition. Therefore, general partial repetition benefits in terms of performance accuracy after re-encountering of at least one feature decrease with age. This suggests a gradual development of lesser reliance on processes that are associated with automatic retrieval or motor execution for event coding. However, general partial repetition costs, reflecting more difficult un-/rebinding and control processes after response alternation, did not vary as a function of age. Accuracy was previously shown to be a more robust and sensitive measure than RT data, specifically in children (Hommel et al., 2011; Karbach et al., 2011). This could explain the lack of age effects in the current RT data. However, when considering development in the other end of the life span it needs to be noted that younger participants tended to commit more errors and consequently to have prolonged experiments than older participants. Long lasting experiments potentially influence fatigue, motivation and data quality. Therefore, future studies are encouraged to separate the age-effect from a potential confounder of task length. Nonetheless, the finding that binding effects are stronger in children than adults was also found in an earlier study (Hommel et al., 2011). Hommel and colleagues compared a group of children (aged 9–10) with adults (20–31) and older adults (64–76). In our current study, a larger cohort of participants distributed in age between 10–30 years was investigated. Using age as a continuous variable allows us to more closely explore the effects of age on event file coding across the studied age range. Over and above replicating previous findings, the current study therefore provides deeper insights into the developmental dynamics of binding during maturation, showing that children were stronger stimulus-response binders and that feature binding and response execution processes change with age. Most importantly, these developmental differences in event file binding observed at the behavioural level were systematically related to neurophysiological markers of event file processing.

Considering neurophysiological processes in developmental studies, it is crucial to note the significance of intra-individual variability in behavioural performance and in EEG data known to change across the lifespan (Bodmer et al., 2017; Li et al., 2004; Papenberg et al., 2013). This was one reason why we analysed RIDE-decomposed data, which showed more reliable results than standard ERP in developmental studies (Bodmer et al., 2017; Giller et al., 2019). In addition to controlling for age-related differences in intra-individual variability, RIDE also allowed us to differentiate underlying event file coding sub-processes. In line with previous studies (Kleimaker et al., 2020; Petruo et al., 2016; Takacs et al., 2020a, 2020b), the C-cluster and the P3 ERP component reflected event file binding processes during which stimulus-response association are retrieved and updated. C-cluster amplitudes in the P3 time window revealed a feature overlap by response interaction. This is consistent with previous research by our group (Kleimaker et al., 2020; Opitz et al., 2020; Takacs et al., 2020a, 2020b). In the current study, amplitudes were smaller when all stimuli and the response were repeated compared to the more difficult condition in which no stimulus was repeated. This condition was represented by faster RTs and higher accuracy scores at the behavioural level, reflecting better performance compared to the more difficult conditions in which unbinding and re-binding of at least one new stimulus leads to partial repetition costs. In the current experimental setting, large C-cluster

amplitudes, just as the P3, apparently correspond to increasing difficulties of selecting the appropriate response (Petruo et al., 2016; Takacs et al., 2020b). Interestingly, no amplitude modulation was seen in the response alternation condition. This is in accordance with Takacs et al. (2020b), suggesting that full feature overlap with an alternating response supressed any response selection capacities, which explains low performance at the behavioural level. The literature on the P3 component is very extensive in exploring the meaning of either increased or decreased amplitudes. Generally, P3 amplitudes become larger with unexpected, unusual targets or when subjects devote more effort to a (difficult) task, but they decrease with increasing uncertainty (Luck, 2014). Similarly, repetition of objects showed to evoke a reduced positivity, reflecting adaptation and enhanced stimulus processing efficiency (Grill-Spector et al., 2006; Stefanics et al., 2018). While reduced neural activity was found to increase with better performance (Grill--Spector et al., 2006), enhanced activity was linked to the presentation of novel stimuli and was more pronounced in children (Nordt et al., 2016). These studies show that reduced C-cluster amplitudes might reflect more efficient processes, due to easier task conditions, learning or adaptation and this effect could improve with age as will be discussed later.

In the current study, the interaction of feature overlap by response in the R-cluster showed different effects than in the C-cluster: amplitudes increased for the repeating features (i.e. full overlaps) and repeating response condition but decreased for the repeating features and alternation condition. Therefore, amplitudes decreased with more demanding response selections processes but increased with better response selection capacities. Because we were interested in event-file coding processes and not in mere response-related processes, the R-cluster activity was measured in the P3 time interval after stimulus presentation, just as the C-cluster. The different results in both clusters show that the interaction effect in the R-cluster might be attributed to processes that are independent of the C-cluster and rather reflect motor control processes (Chmielewski et al., 2019; Friedrich and Beste, 2020; Ouyang et al., 2015, 2011). The S-cluster did not reveal any interaction effects. This is consistent with previous findings showing that stimulus-related processes, as reflected in the S-cluster, do not mirror event file coding processes (Ouyang et al., 2011, 2015; Takacs et al., 2020b). The S-cluster might rather reflect object-file processes that share portions of the event file but change independently of stimulus-response associations (Hommel et al., 2001).

A key novel finding emerged from the analysis integrating (correlating) RIDE-decomposed EEG components and age. Specifically, we could show that there was a linear correlation between age and event file binding effects both in the C- and in the R-cluster. Against the background that at the behavioural level the strength of binding, i.e. the difference between the full feature minus the no feature overlap condition, decreased with age, we examined amplitude modulations between both overlapping feature conditions depending on age. In the C-cluster, our findings revealed a negative correlation between mean amplitude modulation and increasing age for both response types. In contrast to the behavioural data, in which age effects were only visible in the repetition condition, the neurophysiological data yielded age-dependent mechanisms in the two response conditions and therefore showed effects regarding both partial repetition benefits and costs. As reflected by increased repetition benefits in children at the behavioural level, C-cluster modulation effects in the repetition condition might incorporate decreased automatic retrieval and motor execution processes with increasing age. Although the behavioural data did not show age-dependent repetition costs, activation modulation in the C-cluster within the alternation condition reflects more demanding event-file updating and control processes with increasing age. This is consistent with the notion that the C-cluster entails stimulus-response associations and response selection processes (Ouyang et al., 2017; Verleger et al., 2014; Wolff et al., 2017). The C-cluster modulation is also in accordance with the idea that a neural positivity after stimulus repetition is enhanced in children (Nordt et al., 2016) but decreases with better performance efficiency (Grill-Spector et al., 2006; Luck, 2014; Stefanics et al., 2018). In the same way, amplitude modulation after stimulus-response binding could therefore reflect maturational processes. In contrast, the R-cluster showed a positive age correlation in the alternation condition only. The opposite directions of the correlations indicate that the underlying mechanisms in the C-cluster and R-cluster represent different mechanisms of event file coding. As suggested by various other data (Bodmer et al., 2018; Ouyang et al., 2015), the R-cluster might reflect motor-related processes. Apparently, brain responses depending on overlapping feature levels are differently and gradually modulated from late childhood into early adulthood. While neurophysiological modulation in the C-cluster reflects more efficient response selection and stimulus-response updating processes from childhood to early adulthood (i.e., smaller amplitudes suffice for better performance in older ages), the underlying component reflected in the R-cluster is associated with strengthened response inhibition processes with increasing age (i.e. higher amplitudes for better performance in older adults).

At the source level, the correlations both in the C- and in the R-cluster were mirrored by activity modulations in the superior parietal cortex (BA7) which has previously been linked to event coding in numerous studies (Chmielewski et al., 2019; Friedrich and Beste, 2020; Gottlieb, 2007; Kleimaker et al., 2020; Le et al., 2017; Mückschel et al., 2017; Petruo et al., 2016; Takacs et al., 2020b). In some studies, binding effects were reflected by the P3 component or the C-cluster and were related to the inferior parietal cortex (BA40) (Kleimaker et al., 2020; Petruo et al., 2016; Takacs et al., 2020b). The function of binding sensory, motor and cognitive information into a topographically organized salient representation has been attributed to this area (Gottlieb, 2007), which fits to the stimulus-response binding concept of TEC (Hommel et al., 2001). However, aside from the C-cluster, developmental effects in the R-cluster were also associated with BA7. As mentioned, a central aspect in event file coding is to associate stimuli with the appropriate response. Importantly, this means that response options that are not correct have to be discarded. This requires some form of inhibitory control. Indeed, multiple research findings suggest that superior parietal inhibitory mechanisms contribute in the selection of motor responses (Bernier et al., 2012; Cisek and Kalaska, 2002; Jaffard et al., 2008; Sulpizio et al., 2017) and recent findings suggest that R-cluster modulations associated with superior parietal activity may reflect inhibitory control of motor response options (Chmielewski et al., 2019; Friedrich and Beste, 2020). In the current study, correlations of age and R-cluster data were evident in the time period between ~400 and 450 ms. Since the mean reaction times were consistently longer than ~525 ms (cf. Fig. 2), it is well possible that observed dynamics reflect inhibitory control of response options preceding the overt motor response. We suggest that age-related modulations of the binding processes found at parietal regions in the R-cluster reflect inhibitory control subprocesses subserving the selection of the appropriate motor programme amongst competing response options. **Regarding this functional interpretation, it needs to be acknowledged that due to the inverse problem in EEG data, the source localization results are not as definite as it would have been the case with fMRI data. Therefore, the functional interpretation of the sLORETA findings needs to be cautious. However, recent data on developmental effects in binding processes within the motor domain (Dilcher et al., 2021) in the same age range was also associated with the superior parietal cortex (BA7). Therefore, it seems that processes subserving 'binding' in various contexts is a function of superior parietal cortices. This consistency of findings lends support to the reliability of source localization results and their conceptual validity.**

Interestingly, the role of the parietal cortex for cognitive changes during development has been demonstrated in numerous studies (Andre et al., 2016; Darki and Klingberg, 2015; Luna et al., 2010; Ofen et al., 2012; Shing et al., 2010; van Duijvenvoorde et al., 2016). For instance, fronto-parietal networks and parietal regions have been suggested to be

associated with maturational processes in cognition, such as working memory, executive function or memory retrieval (Andre et al., 2016; Crone and Richard Ridderinkhof, 2011; Li et al., 2006; Luna et al., 2010; Ofen et al., 2012; Shing et al., 2010; van Duijvenvoorde et al., 2016). Specifically, activation in the superior parietal cortex (BA7) increased with age and was related to functional maturation of working memory or memory retrieval (Andre et al., 2016; Ofen et al., 2012). Despite the fact that developmental changes in cognitive control and inhibitory control were more attributed to the prefrontal cortex, there is general agreement that modulatory brain changes are associated with cognitive control improvements with age (Andre et al., 2016; Crone, 2014; Crone and Steinbeis, 2017; Darki and Klingberg, 2015; Hämmerer et al., 2014; Li, 2012; Luna et al., 2010). Furthermore, increases in the strength and amount of connections between distributed brain areas during maturation allow more efficient interaction between distant regions (Luna et al., 2010; Shing et al., 2010). Given that long-range information processing networks and the dopaminergic system are related to event file coding in particular (Colzato et al., 2007a, 2007b, 2012, 2013; Colzato and Hommel, 2008; Petruo et al., 2016; Takacs et al., 2020b), maturation of those systems might explain the increased event file updating and inhibitory control abilities with increasing age in our study. During development, some brain regions may be better specialized or focalized and cognitive processes could shift from one area to another (Crone and Richard Ridderinkhof, 2011; Shing et al., 2010). This could explain why brain regions are differently engaged in children and adulthood and why adults rely more on parietal regions rather than solely on prefrontal regions during event coding. However, it needs to be underscored that age-related effects based on cross-sectional age samples, albeit covering a broad age range and not focusing on extreme age groups as the case here, are only proxies of age-related changes at best and could not inform causal relations between brain changes and performance (Raz & Lindenberger, 2011; Lindenberger & Pötter, 1998), Thus, longitudinal studies that assess the development of event-file coding at the behavioural and brain levels need to be conducted in the future to more directly examine the impacts of maturational changes in the frontal-parietal network on the development of event-file coding.

5. Conclusion

This study provided novel insights into the neurophysiological dynamics underlying the development of event file coding that may reflect the gradual maturation of the frontal-parietal network. The behavioural results revealed that performance accuracy differences between feature overlap levels decreased with age. Therefore, event file updating processes become more efficient from late childhood to early adulthood in a linear fashion. These binding effects are reflected by two neurophysiological subprocesses associated with the superior parietal cortex (BA7) as revealed by EEG signal decomposition. The first process refers to mapping and association processes between stimulus and response, the second refers to processes involved in inhibitory control subprocesses subserving the selection of the appropriate motor programme amongst competing response options.

Data and code availability statement

The anonymized data reported in the study and the associated data analysis codes can be made available for other researchers upon request sent to the corresponding authors. This procedure complies with the requirements of our funding agents and the institutional ethics approval.

Declaration of Competing Interest

The authors declare that they have no known competing financial interests or personal relationships that could have appeared to influence the work reported in this paper.

Acknowledgements

This work was supported by a Grant from the Deutsche Forschungsgemeinschaft (DFG) FOR 2698. Shu-Chen Li was also supported by the Excellence Strategy of the DFG (EXC 2050/1 – Project ID 390696704).

Appendix A. Supplementary data

Supplementary material related to this article can be found, in the online version, at doi:https://doi.org/10.1016/j.dcn.2021.100977.

References

Andre, J., Picchioni, M., Zhang, R., Toulopoulou, T., 2016. Working memory circuit as a function of increasing age in healthy adolescence: a systematic review and meta-analyses. Neuroimage Clin. 12, 940–948. https://doi.org/10.1016/j.nicl.2015.12.002.

Arnsten, A.F.T., Rubia, K., 2012. Neurobiological circuits regulating attention, cognitive control, motivation, and emotion: disruptions in neurodevelopmental psychiatric disorders. J. Am. Acad. Child Adolesc. Psychiatry 51, 356–367. https://doi.org/10.1016/j.jaac.2012.01.008.

Bäckman, L., Nyberg, L., Lindenberger, U., Li, S.-C., Farde, L., 2006. The correlative triad among aging, dopamine, and cognition: current status and future prospects. Neurosci. Biobehav. Rev. 30, 791–807. https://doi.org/10.1016/j.neubiorev.2006.06.005.

Bernier, P.-M., Cieslak, M., Grafton, S.T., 2012. Effector selection precedes reach planning in the dorsal parietofrontal cortex. J. Neurophysiol. 108, 57–68. https://doi.org/10.1152/jn.00011.2012.

Beste, C., Tübing, J., Seeliger, H., Bäumer, T., Brandt, V., Stock, A.-K., Münchau, A., 2016. Altered perceptual binding in Gilles de la Tourette syndrome. Cortex 83, 160–166. https://doi.org/10.1016/j.cortex.2016.07.015.

Bodmer, B., Mückschel, M., Roessner, V., Beste, C., 2017. Neurophysiological variability masks differences in functional neuroanatomical networks and their effectiveness to modulate response inhibition between children and adults. Brain Struct. Funct. https://doi.org/10.1007/s00429-017-1589-6.

Bodmer, B., Mückschel, M., Roessner, V., Beste, C., 2018. Neurophysiological variability masks differences in functional neuroanatomical networks and their effectiveness to modulate response inhibition between children and adults. Brain Struct. Funct. 223, 1797–1810. https://doi.org/10.1007/s00429-017-1589-6.

Chmielewski, W., Bluschke, A., Bodmer, B., Wolff, N., Roessner, V., Beste, C., 2019. Evidence for an altered architecture and a hierarchical modulation of inhibitory control processes in ADHD. Dev. Cogn. Neurosci. 36, 100623 https://doi.org/10.1016/j.dcn.2019.100623.

Cisek, P., Kalaska, J.F., 2002. Modest gaze-related discharge modulation in monkey dorsal premotor cortex during a reaching task performed with free fixation. J. Neurophysiol. 88, 1064–1072. https://doi.org/10.1152/jn.00995.2001.

Colzato, L.S., Hommel, B., 2008. Cannabis, cocaine, and visuomotor integration: Evidence for a role of dopamine D1 receptors in binding perception and action. Neuropsychologia 46, 1570–1575. https://doi.org/10.1016/j.neuropsychologia.2007.12.014.

Colzato, L.S., Warrens, M.J., Hommel, B., 2006. Priming and binding in and across perception and action: a correlational analysis of the internal structure of event files. Q. J. Exp. Psychol. 59, 1785–1804. https://doi.org/10.1080/17470210500438304.

Colzato, L.S., van Wouwe, N.C., Hommel, B., 2007a. Feature binding and affect: Emotional modulation of visuo-motor integration. Neuropsychologia 45, 440–446. https://doi.org/10.1016/j.neuropsychologia.2006.06.032.

Colzato, L.S., van Wouwe, N.C., Hommel, B., 2007b. Spontaneous eyeblink rate predicts the strength of visuomotor binding. Neuropsychologia 45, 2387–2392. https://doi.org/10.1016/j.neuropsychologia.2007.03.004.

Colzato, L.S., van Wouwe, N.C., Hommel, B., Zmigrod, S., Ridderinkhof, K.R., Wylie, S. A., 2012. Dopaminergic modulation of the updating of stimulus–response episodes in Parkinson's disease. Behav. Brain Res. 228, 82–86. https://doi.org/10.1016/j.bbr.2011.11.034.

Colzato, L.S., Zmigrod, S., Hommel, B., 2013. Dopamine, norepinephrine, and the management of sensorimotor bindings: individual differences in updating of stimulus–response episodes are predicted by DAT1, but not DBH5′-ins/del. Exp. Brain Res. 228, 213–220. https://doi.org/10.1007/s00221-013-3553-x.

Crone, E.A., 2014. The role of the medial frontal cortex in the development of cognitive and social-affective performance monitoring: performance monitoring in adolescence. Psychophysiology 51, 943–950. https://doi.org/10.1111/psyp.12252.

Crone, E.A., Richard Ridderinkhof, K., 2011. The developing brain: from theory to neuroimaging and back. Dev. Cogn. Neurosci. 1, 101–109. https://doi.org/10.1016/j.dcn.2010.12.001.

Crone, E.A., Steinbeis, N., 2017. Neural perspectives on cognitive control development during childhood and adolescence. Trends Cogn. Sci. 21, 205–215. https://doi.org/10.1016/j.tics.2017.01.003.

Crone, E.A., Bunge, S.A., van der Molen, M.W., Ridderinkhof, K.R., 2006. Switching between tasks and responses: a developmental study. Dev. Sci. 9, 278–287. https://doi.org/10.1111/j.1467-7687.2006.00490.x.

Darki, F., Klingberg, T., 2015. The Role of Fronto-Parietal and Fronto-Striatal Networks in the Development of Working Memory: A Longitudinal Study. Cereb. Cortex 25, 1587–1595. https://doi.org/10.1093/cercor/bht352.
Diamond, A., 2013. Executive functions. Annu. Rev. Psychol. 64, 135–168. https://doi.org/10.1146/annurev-psych-113011-143750.
Dilcher, R., Jamous, R., Takacs, A., Tóth-Fáber, E., Münchau, A., Li, S.-C., Beste, C., 2021. Neurophysiology of embedded response plans: age effects in action execution but not in feature integration from preadolescence to adulthood. J. Neurophysiol. 125, 1382–1395. https://doi.org/10.1152/jn.00681.2020.
Dippel, G., Beste, C., 2015. A causal role of the right inferior frontal cortex in implementing strategies for multi-component behaviour. Nat. Commun. 6, 6587. https://doi.org/10.1038/ncomms7587.
Freund, M.C., Etzel, J.A., Braver, T.S., 2021. Neural coding of cognitive control: the representational similarity analysis approach. Trends Cogn. Sci. https://doi.org/10.1016/j.tics.2021.03.011.
Friedman, D., Nessler, D., Cycowicz, Y.M., Horton, C., 2009. Development of and change in cognitive control: a comparison of children, young adults, and older adults. Cogn. Affect. Behav. Neurosci. 9, 91–102. https://doi.org/10.3758/CABN.9.1.91.
Friedrich, J., Beste, C., 2020. Low and high stimulation frequencies differentially affect automated response selection in the superior parietal cortex – implications for somatosensory area processes. Sci. Rep. 10, 3954. https://doi.org/10.1038/s41598-020-61025-y.
Frings, C., Hommel, B., Koch, I., Rothermund, K., Dignath, D., Giesen, C., Kiesel, A., Kunde, W., Mayr, S., Moeller, B., Möller, M., Pfister, R., Philipp, A., 2020. Binding and retrieval in action control (BRAC). Trends Cogn. Sci. 24, 375–387. https://doi.org/10.1016/j.tics.2020.02.004.
Fuchs, M., Kastner, J., Wagner, M., Hawes, S., Ebersole, J.S., 2002. A standardized boundary element method volume conductor model. Clin. Neurophysiol. Off. J. Int. Fed. Clin. Neurophysiol. 113, 702–712.
Giller, F., Zhang, R., Roessner, V., Beste, C., 2019. The neurophysiological basis of developmental changes during sequential cognitive flexibility between adolescents and adults. Hum. Brain Mapp. 40, 552–565. https://doi.org/10.1002/hbm.24394.
Gottlieb, J., 2007. From thought to action: the parietal cortex as a bridge between perception, action, and cognition. Neuron 53, 9–16. https://doi.org/10.1016/j.neuron.2006.12.009.
Grill-Spector, K., Henson, R., Martin, A., 2006. Repetition and the brain: neural models of stimulus-specific effects. Trends Cogn. Sci. 10, 14–23. https://doi.org/10.1016/j.tics.2005.11.006.
Hämmerer, D., Müller, V., Li, S.-C., 2014. Performance monitoring across the lifespan: still maturing post-conflict regulation in children and declining task-set monitoring in older adults. Neurosci. Biobehav. Rev. 46, 105–123. https://doi.org/10.1016/j.neubiorev.2014.06.008.
Hommel, B., 1998. Event files: evidence for automatic integration of stimulus-response episodes. Vis. Cogn. 5, 183–216. https://doi.org/10.1080/713756773.
Hommel, B., 2009. Action control according to TEC (theory of event coding). Psychol. Res. Psychol. Forsch. 73, 512–526. https://doi.org/10.1007/s00426-009-0234-2.
Hommel, B., Müsseler, J., Aschersleben, G., Prinz, W., 2001. The Theory of Event Coding (TEC): a framework for perception and action planning. Behav. Brain Sci. 24, 849–878. https://doi.org/10.1017/S0140525X01000103.
Hommel, B., Kray, J., Lindenberger, U., 2011. Feature Integration Across the Lifespan: Stickier Stimulus?Response Bindings in Children and Older Adults. Front. Psychol. 2 https://doi.org/10.3389/fpsyg.2011.00268.
Jaffard, M., Longcamp, M., Velay, J.-L., Anton, J.-L., Roth, M., Nazarian, B., Boulinguez, P., 2008. Proactive inhibitory control of movement assessed by event-related fMRI. NeuroImage 42, 1196–1206. https://doi.org/10.1016/j.neuroimage.2008.05.041.
Jucaite, A., Forssberg, H., Karlsson, P., Halldin, C., Farde, L., 2010. Age-related reduction in dopamine D1 receptors in the human brain: from late childhood to adulthood, a positron emission tomography study. Neuroscience 167, 104–110. https://doi.org/10.1016/j.neuroscience.2010.01.034.
Karbach, J., Kray, J., Hommel, B., 2011. Action–effect learning in early childhood: does language matter? Psychol. Res. 75, 334–340. https://doi.org/10.1007/s00426-010-0308-1.
Kayser, J., Tenke, C.E., 2015. On the benefits of using surface Laplacian (current source density) methodology in electrophysiology. Int. J. Psychophysiol. 97, 171–173. https://doi.org/10.1016/j.ijpsycho.2015.06.001.
Kikumoto, A., Mayr, U., 2020. Conjunctive representations that integrate stimuli, responses, and rules are critical for action selection. Proc. Natl. Acad. Sci. 117, 10603–10608. https://doi.org/10.1073/pnas.1922166117.
Kleimaker, M., Takacs, A., Conte, G., Onken, R., Verrel, J., Bäumer, T., Münchau, A., Beste, C., 2020. Increased perception-action binding in Tourette syndrome. Brain, awaa111. https://doi.org/10.1093/brain/awaa111.
Klimesch, W., 2011. Evoked alpha and early access to the knowledge system: the P1 inhibition timing hypothesis. Brain Res. 1408, 52–71. https://doi.org/10.1016/j.brainres.2011.06.003.
Kray, J., Eber, J., Karbach, J., 2008. Verbal self-instructions in task switching: a compensatory tool for action-control deficits in childhood and old age? Dev. Sci. 11, 223–236. https://doi.org/10.1111/j.1467-7687.2008.00673.x.
Le, A., Vesia, M., Yan, X., Crawford, J.D., Niemeier, M., 2017. Parietal area BA7 integrates motor programs for reaching, grasping, and bimanual coordination. J. Neurophysiol. 117, 624–636. https://doi.org/10.1152/jn.00299.2016.
Li, S.-C., 2012. Neuromodulation of behavioral and cognitive development across the life span. Dev. Psychol. 48, 810–814. https://doi.org/10.1037/a0027813.
Li, S.-C., Lindenberger, U., Hommel, B., Aschersleben, G., Prinz, W., Baltes, P.B., 2004. Transformations in the couplings among intellectual abilities and constituent cognitive processes across the life span. Psychol. Sci. 15, 155–163. https://doi.org/10.1111/j.0956-7976.2004.01503003.x.
Li, S.-C., Brehmer, Y., Shing, Y.L., Werkle-Bergner, M., Lindenberger, U., 2006. Neuromodulation of associative and organizational plasticity across the life span: Empirical evidence and neurocomputational modeling. Neurosci. Biobehav. Rev. 30, 775–790. https://doi.org/10.1016/j.neubiorev.2006.06.004.
Luck, S.J., 2014. An Introduction to the Event-related Potential Technique, second edition. The MIT Press, Cambridge, Massachusetts.
Luna, B., 2009. Developmental changes in cognitive control through adolescence. Adv. Child Dev. Behav. 37, 233–278. https://doi.org/10.1016/s0065-2407(09)03706-9.
Luna, B., Padmanabhan, A., O'Hearn, K., 2010. What has fMRI told us about the development of cognitive control through adolescence? Brain Cogn. 72, 101–113. https://doi.org/10.1016/j.bandc.2009.08.005.
Marco-Pallarés, J., Grau, C., Ruffini, G., 2005. Combined ICA-LORETA analysis of mismatch negativity. NeuroImage 25, 471–477. https://doi.org/10.1016/j.neuroimage.2004.11.028.
Marek, S., Hwang, K., Foran, W., Hallquist, M.N., Luna, B., 2015. The contribution of network organization and integration to the development of cognitive control. PLoS Biol. 13, e1002328 https://doi.org/10.1371/journal.pbio.1002328.
Mazziotta, J., Toga, A., Evans, A., Fox, P., Lancaster, J., Zilles, K., Woods, R., Paus, T., Simpson, G., Pike, B., Holmes, C., Collins, L., Thompson, P., MacDonald, D., Iacoboni, M., Schormann, T., Amunts, K., Palomero-Gallagher, N., Geyer, S., Parsons, L., Narr, K., Kabani, N., Le Goualher, G., Boomsma, D., Cannon, T., Kawashima, R., Mazoyer, B., 2001. A probabilistic atlas and reference system for the human brain: international Consortium for Brain Mapping (ICBM). Philos. Trans. R. Soc. Lond. Ser. B 356, 1293–1322. https://doi.org/10.1098/rstb.2001.0915.
McTeague, L.M., Huemer, J., Carreon, D.M., Jiang, Y., Eickhoff, S.B., Etkin, A., 2017. Identification of Common Neural Circuit Disruptions in Cognitive Control Across Psychiatric Disorders. Am. J. Psychiatry 174, 676–685. https://doi.org/10.1176/appi.ajp.2017.16040400.
Mückschel, M., Dippel, G., Beste, C., 2017. Distinguishing stimulus and response codes in theta oscillations in prefrontal areas during inhibitory control of automated responses: Distinguishing Stimulus and Response Codes in Theta Oscillations. Hum. Brain Mapp. 38, 5681–5690. https://doi.org/10.1002/hbm.23757.
Munakata, Y., Snyder, H.R., Chatham, C.H., 2012. Developing cognitive control: three key transitions. Curr. Dir. Psychol. Sci. 21, 71–77. https://doi.org/10.1177/0963721412436807.
Nigg, J.T., 2017. Annual Research Review: on the relations among self-regulation, self-control, executive functioning, effortful control, cognitive control, impulsivity, risk-taking, and inhibition for developmental psychopathology. J. Child Psychol. Psychiatry 58, 361–383. https://doi.org/10.1111/jcpp.12675.
Nordt, M., Hoehl, S., Weigelt, S., 2016. The use of repetition suppression paradigms in developmental cognitive neuroscience. Cortex 80, 61–75. https://doi.org/10.1016/j.cortex.2016.04.002.
Ocklenburg, S., Friedrich, P., Fraenz, C., Schlüter, C., Beste, C., Güntürkün, O., Genç, E., 2018. Neurite architecture of the planum temporale predicts neurophysiological processing of auditory speech. Sci. Adv. 4, eaar6830 https://doi.org/10.1126/sciadv.aar6830.
Ofen, N., Chai, X.J., Schuil, K.D.I., Whitfield-Gabrieli, S., Gabrieli, J.D.E., 2012. The development of brain systems associated with successful memory retrieval of scenes. J. Neurosci. 32, 10012–10020. https://doi.org/10.1523/JNEUROSCI.1082-11.2012.
Opitz, A., Beste, C., Stock, A.-K., 2020. Using temporal EEG signal decomposition to identify specific neurophysiological correlates of distractor-response bindings proposed by the theory of event coding. NeuroImage 209, 116524. https://doi.org/10.1016/j.neuroimage.2020.116524.
Ouyang, G., Herzmann, G., Zhou, C., Sommer, W., 2011. Residue iteration decomposition (RIDE): a new method to separate ERP components on the basis of latency variability in single trials: RIDE: a new method to separate ERP components. Psychophysiology 48, 1631–1647. https://doi.org/10.1111/j.1469-8986.2011.01269.x.
Ouyang, G., Sommer, W., Zhou, C., 2015. A toolbox for residue iteration decomposition (RIDE)—A method for the decomposition, reconstruction, and single trial analysis of event related potentials. J. Neurosci. Methods 250, 7–21. https://doi.org/10.1016/j.jneumeth.2014.10.009.
Ouyang, G., Hildebrandt, A., Sommer, W., Zhou, C., 2017. Exploiting the intra-subject latency variability from single-trial event-related potentials in the P3 time range: a review and comparative evaluation of methods. Neurosci. Biobehav. Rev. 75, 1–21. https://doi.org/10.1016/j.neubiorev.2017.01.023.
Papenberg, G., Hämmerer, D., Müller, V., Lindenberger, U., Li, S.-C., 2013. Lower theta inter-trial phase coherence during performance monitoring is related to higher reaction time variability: a lifespan study. NeuroImage 83, 912–920. https://doi.org/10.1016/j.neuroimage.2013.07.032.
Pascual-Marqui, R.D., 2002. Standardized low-resolution brain electromagnetic tomography (sLORETA): technical details. Methods Find. Exp. Clin. Pharmacol. 24 (Suppl D), 5–12.
Petruo, V.A., Stock, A.-K., Münchau, A., Beste, C., 2016. A systems neurophysiology approach to voluntary event coding. NeuroImage 135, 324–332. https://doi.org/10.1016/j.neuroimage.2016.05.007.
Petruo, V., Bodmer, B., Brandt, V.C., Baumung, L., Roessner, V., Münchau, A., Beste, C., 2019. Altered perception-action binding modulates inhibitory control in Gilles de la Tourette syndrome. J. Child Psychol. Psychiatry 60, 953–962. https://doi.org/10.1111/jcpp.12938.
Sekihara, K., Sahani, M., Nagarajan, S.S., 2005. Localization bias and spatial resolution of adaptive and non-adaptive spatial filters for MEG source reconstruction. NeuroImage 25, 1056–1067. https://doi.org/10.1016/j.neuroimage.2004.11.051.
Shing, Y.L., Werkle-Bergner, M., Brehmer, Y., Müller, V., Li, S.-C., Lindenberger, U., 2010. Episodic memory across the lifespan: the contributions of associative and

strategic components. Neurosci. Biobehav. Rev. 34, 1080–1091. https://doi.org/10.1016/j.neubiorev.2009.11.002.
Stefanics, G., Heinzle, J., Czigler, I., Valentini, E., Stephan, K.E., 2018. Timing of repetition suppression of event-related potentials to unattended objects. Eur. J. Neurosci. https://doi.org/10.1111/ejn.13972.
Stock, A.-K., Gohil, K., Huster, R.J., Beste, C., 2017. On the effects of multimodal information integration in multitasking. Sci. Rep. 7, 4927. https://doi.org/10.1038/s41598-017-04828-w.
Sulpizio, V., Lucci, G., Berchicci, M., Galati, G., Pitzalis, S., Di Russo, F., 2017. Hemispheric asymmetries in the transition from action preparation to execution. NeuroImage 148, 390–402. https://doi.org/10.1016/j.neuroimage.2017.01.009.
Takacs, A., Mückschel, M., Roessner, V., Beste, C., 2020a. Decoding stimulus-response representations and their stability using EEG-based multivariate pattern analysis. Cereb. Cortex Commun., tgaa016 https://doi.org/10.1093/texcom/tgaa016.
Takacs, A., Zink, N., Wolff, N., Münchau, A., Mückschel, M., Beste, C., 2020b. Connecting EEG signal decomposition and response selection processes using the theory of event coding framework. Hum. Brain Mapp., hbm.24983 https://doi.org/10.1002/hbm.24983.
van Duijvenvoorde, A.C.K., Achterberg, M., Braams, B.R., Peters, S., Crone, E.A., 2016. Testing a dual-systems model of adolescent brain development using resting-state connectivity analyses. NeuroImage 124, 409–420. https://doi.org/10.1016/j.neuroimage.2015.04.069.
Vedechkina, M., Borgonovi, F., 2021. A review of evidence on the role of digital technology in shaping attention and cognitive control in children. Front. Psychol. 12, 611155 https://doi.org/10.3389/fpsyg.2021.611155.
Verleger, R., Metzner, M.F., Ouyang, G., Śmigasiewicz, K., Zhou, C., 2014. Testing the stimulus-to-response bridging function of the oddball-P3 by delayed response signals and residue iteration decomposition (RIDE). NeuroImage 100, 271–280. https://doi.org/10.1016/j.neuroimage.2014.06.036.
Wolff, N., Mückschel, M., Beste, C., 2017. Neural mechanisms and functional neuroanatomical networks during memory and cue-based task switching as revealed by residue iteration decomposition (RIDE) based source localization. Brain Struct. Funct. 222, 3819–3831. https://doi.org/10.1007/s00429-017-1437-8.